Nuclear Instruments and Methods in Physics Research A283 (1989) 544–552
North-Holland, Amsterdam

THE ARGUS MICROVERTEX DRIFT CHAMBER

E. MICHEL and W. SCHMIDT-PARZEFALL
DESY, Hamburg, FRG

R.D. APPUHN, J. BUCHMÜLLER, H. KOLANOSKI, B. KREIMEIER, A. LANGE, T. SIEGMUND and A. WALTHER
*Institut für Physik, Universität Dortmund *, FRG*

K.W. EDWARDS **, R.C. FERNHOLZ [+], H. KAPITZA **, D.B. MacFARLANE [+], M. O'NEILL **, J.A. PARSONS [++], J.D. PRENTICE [++], S.C. SEIDEL [++], G. TSIPOLITIS [+]
Institute of Particle Physics [§], Canada

S. BALL
University of Kansas [§§], Lawrence, KS, USA

A. BABAEV, M. DANILOV and I. TICHOMIROV
Institute of Theoretical and Experimental Physics, Moscow, USSR

The ARGUS collaboration is currently building a new microvertex drift chamber (μVDC) as an upgrade of their detector The μVDC is optimized for B-meson physics at DORIS energies. Important design features are minimal multiple scattering for low-momentum particles and three-dimensional reconstruction of decay vertices with equal resolutions in $r-\phi$ and $r-z$. Vertex resolutions of 15–25 μm are expected. Prototypes of the μVDC have been tested with different gas mixtures at various pressures. Spatial resolutions as small as 20 μm were obtained using CO_2/propane at 4 bar and DME at 1 bar. New readout electronics have been developed for the μVDC aiming at low thresholds for the TDC measurements. Employing a novel idea for noise and cross-talk suppression, which is based on a discrimination against short pulses, very low threshold settings are possible

1. Introduction

The ARGUS detector at the e^+e^- storage ring DORIS II is currently being upgraded with a high-resolution "microvertex drift chamber" (μVDC) [1], with the aim of reconstructing the primary and secondary vertices with a spatial resolution of 15–25 μm. This will significantly improve the performance of ARGUS in the field of B-meson physics.

Most results on B-meson decays have so far been obtained from the investigation of e^+e^- collisions at the energy of the $\Upsilon(4S)$ resonance ($E = 10.58$ GeV) which decays dominantly into $B\bar{B}$ pairs. The advantages of running at the $\Upsilon(4S)$ are a well defined initial state and a high production rate. A disadvantage arises from the fact that this resonance lies very close to the $B\bar{B}$ threshold, leading to the B-mesons being produced nearly at rest. Hence their decay products are isotropically distributed and completely intermixed. Together with the high decay multiplicity this leads to a severe combinatorial background in the reconstruction of B decays.

Presently, this background is reduced using the good particle identification capabilities of ARGUS [2]. Here one exploits the fact that B-mesons decay dominantly into charmed mesons. Particularly clean signals are obtained if the B reconstruction proceeds via the intermediate charmed state D^{*+} [3]. However, the product of several small detection efficiencies and branching ratios is involved in such decay chains, leading to effective B reconstruction efficiencies of less than 10^{-3}.

* Supported by the German Bundesministerium für Forschung und Technologie, under contract 054DO51P
** Carleton University, Ottawa, Ontario, Canada.
[+] McGill University, Montreal, Quebec, Canada
[++] University of Toronto, Ontario, Canada.
[§] Supported by the Natural Sciences and Engineering Research Council, Canada.
[§§] Supported by the US National Science Foundation.

The μVDC will provide independent topological information for reducing the combinatorial background by identifying the decay vertices of charmed mesons. The average flight distances of D^0 and D^+ mesons from B decays on the $\Upsilon(4S)$ resonance are 60 and 115 μm, respectively. With a vertex resolution of 15–25 μm a large fraction of the charm vertices will be resolved. A Monte Carlo study has shown that it is mandatory to achieve this precision in both the r–ϕ and r–z projections (perpendicular to and parallel to the beam axis) in order to efficiently reject faked vertices [1]. Assuming a 50% efficiency for tagging the decay $D^0 \to K^-\pi^+$ via the decay length, a signal-to-background ratio of 1 : 2 was obtained, five times better than presently achieved without tagging. Hence the μVDC would provide clean D^0 and D^+ signals for the subsequent reconstruction of B-mesons, without having to reconstruct the intermediate D^{*+} state.

2. Design of the μVDC

2.1. Choice of the detector type

Most particles from decays of B-mesons produced near threshold have momenta well below 1 GeV/c. In this momentum range the use of silicon strip detectors, which at the time of the μVDC design were only available with a typical thickness of 300 μm per measured coordinate, is ruled out because of the introduction of a large multiple scattering error. Instead, it was concluded that a vertex detector for the proposed application would have to be a gaseous detector. Initially the "radial drift chamber" [4] or "induction drift chamber" [5] principle was proposed for the μVDC. While resolutions as small as 10 μm have been obtained, this holds only for tracks with nearly perpendicular incidence, a condition which is generally not fulfilled in our case.

Instead, the design of the μVDC is based on the conventional drift chamber principle. This decision was supported by reports of resolutions down to 25 μm obtained in drift chambers with pressurized slow gases (CO_2 with isobutane admixtures) [6].

2.2. Wire layer arrangement

The ARGUS μVDC is a cylindrical drift chamber which is designed to fit inside the space available in the inner tube of the main drift chamber (30 cm diameter), and between the two compensation coils (137 cm apart).

The chamber contains 1070 sense wires which are arranged in 16 layers: four layers of axial wires and six pairs of layers with wires at angles of $\pm 45°$ relative to the chamber axis (see table 1). Due to the extremely large stereo angles the track coordinates in the r–ϕ and r–z projections can be measured with equal precision. The axial wires are needed to resolve ambiguities in the pattern recognition process.

A mechanical support structure is needed to guide the stereo wires around the chamber axis. This is accomplished by feeding the wires through holes in five longitudinal plates (so-called vanes) extending between two end cones, as shown schematically in fig. 1.

The end cones are machined from aluminium blocks. On the side of the active chamber volume they have steps designed to accommodate ceramic boards (Macor) on which the sense wires and cathode wires are accurately positioned and fixed (see fig. 2).

The vanes are made of 0.89 mm thick beryllium sheet. This material combines great mechanical stiffness

Table 1
Sense wire layers in the μVDC

Layer	Stereo angle α	r_{max} [mm]	r_{min} [mm]	z_{max} [mm]	Number of cells
1	0°	32.0	25.889	75.237	35
2	0°	38.4	31.066	90.284	40
3	+45°	44.8	36.244	105.331	35
4	−45°	51.2	41.422	120.378	40
5	+45°	57.6	46.599	135.426	45
6	−45°	64.0	51.777	150.473	50
7	+45°	70.4	56.955	165.520	55
8	−45°	76.8	62.133	180.568	60
9	0°	83.2	67.310	195.615	90
10	0°	89.6	72.488	210.662	95
11	+45°	96.0	77.666	225.710	75
12	−45°	102.4	82.843	240.757	80
13	+45°	108.8	88.021	255.804	85
14	−45°	115.2	93.199	270.851	90
15	+45°	121.6	93.376	285.899	95
16	−45°	128.0	103.554	300.946	100

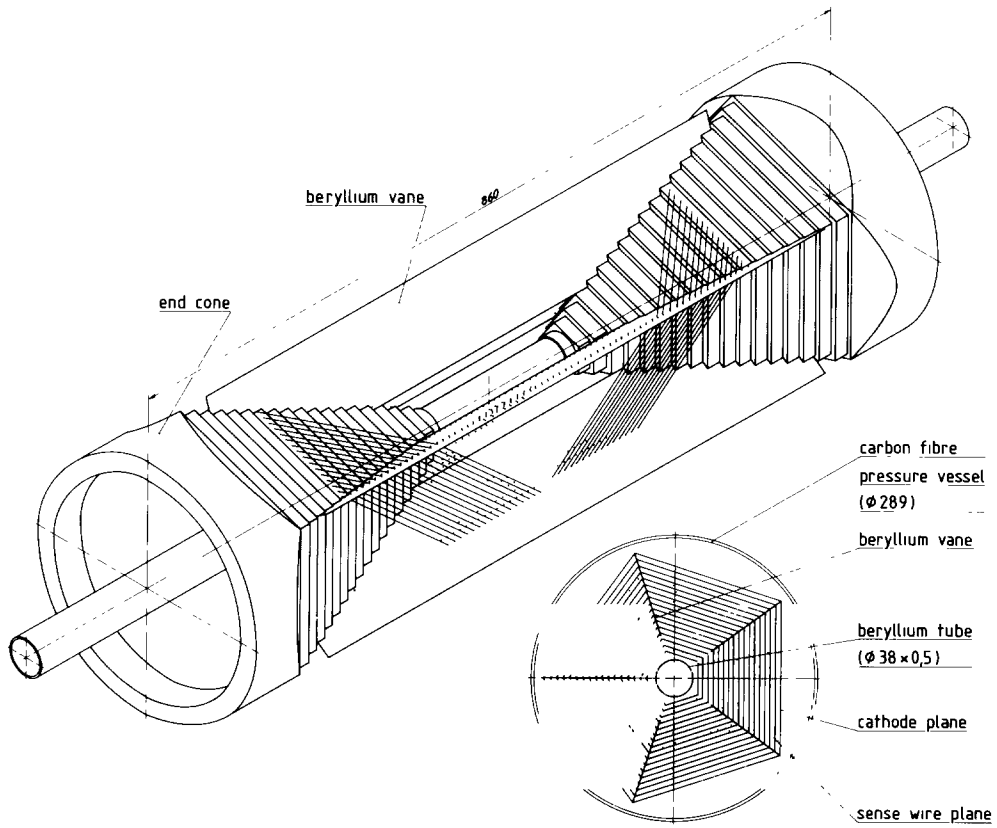

Fig. 1. Schematic view of the μVDC. The sense wires are wrapped around the chamber axis, supported by a structure made of five beryllium plates extending between two aluminium end cones. In each of the five chamber sectors there are 16 sense wire layers with adjacent stereo wire layers crossing at a 90° angle.

with low multiple scattering. Each vane has 672 holes of 2 mm diameter. Into each of these holes a synthetic ruby with a central 380 μm diameter hole is inserted which accurately positions a wire. The vanes are covered with thin layers (25 μm) of Mylar with field-shaping electrodes printed on them. This helps to reduce the inefficient region close to the vanes.

The wire support structure is designed with a mecha-

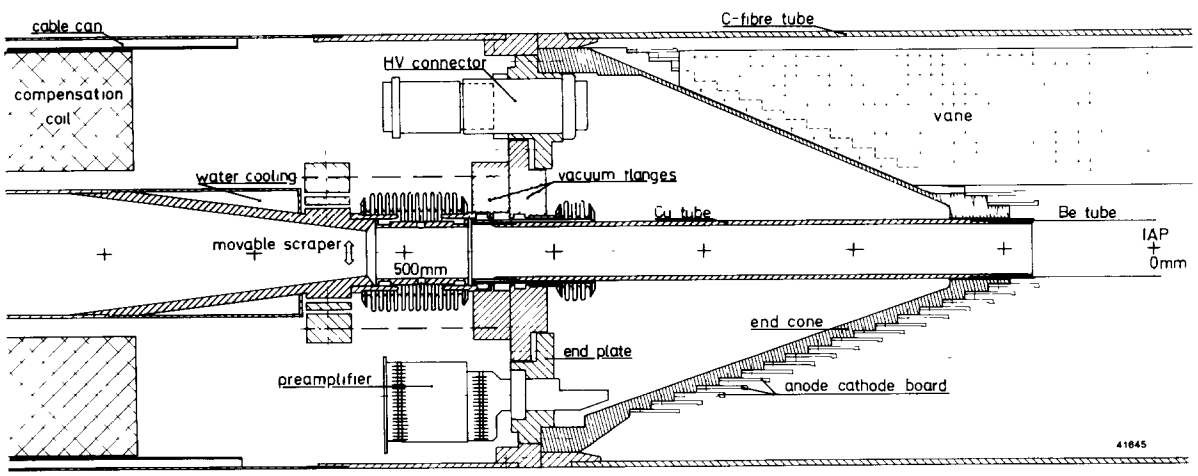

Fig. 2. Section through the μVDC parallel to the beam axis

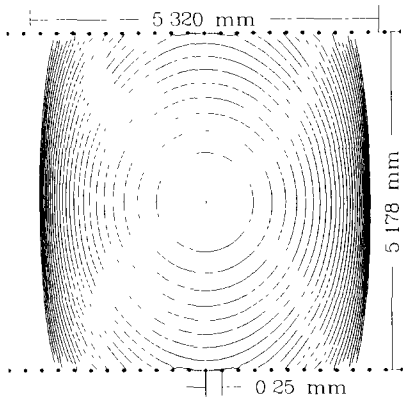

Fig. 3 Design of the μVDC drift cell. Sense wire (open circle) and cathode wires (full circles) are not parallel in the stereo layers. Also shown are the isochrones for CO_2/propane (80/20) at $p = 4$ bar and HV = 4040 V for drift times of 20–520 ns in steps of 20 ns.

nical precision of 25–50 μm, in order to keep gas amplification variations below 1%. The precise wire positions needed to achieve the ultimate resolution will be obtained by a calibration procedure (see section 3.1).

The support structure is designed such that each stereo wire passes through 4 of the 5 vanes. This results in a unique mapping of ϕ- and z-values, which considerably simplifies the data analysis. The solid angle acceptance of the μVDC is $0.93 \times 4\pi$ and matches that of the other components of ARGUS [2]. Approximately 2% of the azimuthal acceptance is shadowed by the vanes.

2.3. Drift cell design

In order to keep the track extrapolation error small, the innermost sense wire layer has a distance of only 25.9 mm from the beam line (see table 1). A reasonable multitrack resolution in B decay events requires about 40 drift cells at the inner radius of the chamber. As a consequence, the drift cells in the μVDC must be small. The distance from one sense wire layer to the next is 5.178 mm, while adjacent sense wires in the same layer are 5.320 mm apart (see fig. 3). All drift cells in the μVDC have the same size.

The sense wires are made of gold-plated tungsten with a diameter of 25 μm. There are no field wires explicitly separating the drift cells, since they too would have to be fed through the vanes, and this was thought to cause HV breakdown problems. On the other hand, leaving out the field wires leads to inefficient regions in the drift cell far from the sense wire due to the extremely slow drift of the electrons (see fig. 3). The properties of small drift cells without field wires have been investigated in prototype tests (see section 3.1).

The sense wire layers are separated by cathode planes consisting of axial stainless steel wires with a diameter of 25 μm and a spacing of 250 μm. This cathode design represents an optimum in terms of acceptable field strength on the wire surface (26 kV/cm for HV = 4040 V) and minimal multiple scattering (on average 0.17% of a radiation length).

2.4. Pressure vessel

In each drift chamber the resolution deteriorates towards the sense wires due to ionization statistics. For small drift cells a relatively large fraction of the total cell area will be affected. This can be compensated by increasing the pressure in the chamber. The μVDC is designed to run at absolute pressures up to 4 bar. The pressure vessel consists of the outer cylinder, the end plates, and the beam pipe (see fig. 2). The outer cylinder is made of a 3.5 mm thick carbon-fibre epoxy composite. The end plates are made of aluminium. They contain pressure-tight feedthroughs for signal and high voltage cables, pressure and temperature sensor lines, and gas input and output connectors.

2.5. Beam pipe and synchrotron radiation absorbers

As noted above, the beam pipe also forms the inner wall of the μVDC. Its central section is a 160 mm long beryllium tube with a 0.5 mm wall thickness and an outer diameter of 38 mm. On each end, 375 mm long copper tubes are brazed to the beryllium (see fig. 2). Multiple scattering in the beryllium tube introduces a 10 μm error at the beam position for 0.5 GeV/c pions.

The beam pipe, with its central beryllium section, must not be subject to any longitudinal forces from the gas pressure or the wire tension. It must also be kept free from mechanical stress when connected to the storage ring vacuum system. These considerations led to the design of a "floating" beam pipe which is coupled to the pressure vessel end plates by means of flexible bellows (see fig. 2). Thus all forces are carried across the outer pressure vessel which is rigidly connected to the vacuum system.

The shielding of synchrotron radiation was investigated in detailed simulation studies. The following optimal solution emerged from these calculations. The direct radiation from the last bends of the storage ring is screened by movable copper collimators with 30 mm apertures on either side of the μVDC. The backscattering radiation from the copper is attenuated by a 50 μm aluminium layer on the inside of the beryllium tube. The fluorescence radiation of the aluminium is absorbed by the beryllium. The collimators as well as the copper parts of the beam pipe will be water-cooled.

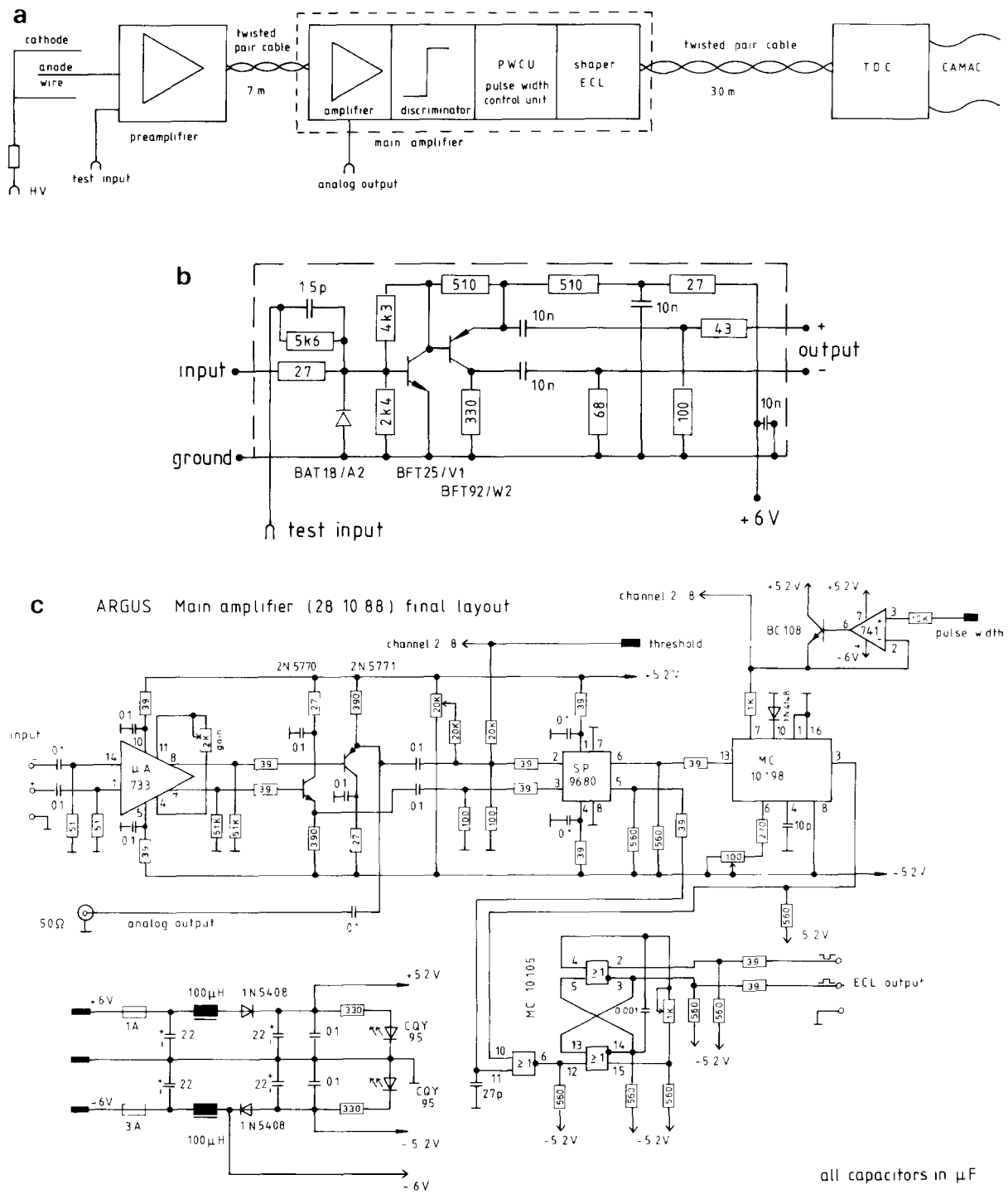

Fig. 4. (a) Readout electronics signal chain for one channel. (b) Preamplifier circuit diagram. (c) Main amplifier circuit diagram.

2.6. Electronics

To some extent the ultimate resolution of the μVDC will be determined by the properties of the readout electronics. The signal processing chain for one channel is shown schematically in fig. 4a.

The current-sensitive preamplifier (fig. 4b) was developed from the circuit currently used for the ARGUS

Table 2
Preamplifier and main amplifier specifications

Preamplifier specifications	
Rise time (10–90%)	3.9 ns
Sensitivity	4 mV/μA
Input impedance	100–140 Ω
Output impedance	100 Ω
Power dissipation	24 mW/channel
Main amplifier specifications	
Net voltage gain	25
Required pulse width	15–100 ns
Cross-talk suppression	> 50 dB
Time stability	< 0.4 ns
Input impedance	100 Ω
Output impedance	100 Ω
Power dissipation	1.25 W/channel

main and vertex drift chambers [2]. Each chamber end plate accommodates 5 blocks of 14 vertically mounted preamplifier cards, each with 8 channels. This high density of channels is achieved by using SMD technology, resulting in a card size of 53.5×43.0 mm^2 and a card spacing of 4.0 mm. The power dissipation is only 24 mW per channel, and the generated heat will be carried away by a simple air cooling system. Some properties of the preamplifiers are listed in table 2.

The drift times will be measured using single hit TDCs (LeCroy System 4290). Under these circumstances, running at low thresholds requires an efficient suppression of noise pulses. The main difference in the shape of anode signals and noise pulses is the pulse width rather than the pulse height. This observation was exploited in the design of the main amplifiers (fig. 4c). For each channel the circuit consists of an amplification stage, a pulse height discriminator, a pulse width control unit (PWCU), and an ECL shaper. The thresholds for pulse height and width can be adjusted externally. The suppression of cross talk between neighbouring channels improves from 40 dB to > 50 dB if the PWCU is used. The main amplifier specifications are listed in table 2. For selected channels the amplified analog signal will be sent to ADCs in order to monitor the gas amplification. The whole system can be calibrated by means of test pulses sent to the preamplifier inputs.

3. Prototype tests

Tests were performed using three different test modules. The modules were designed to fit into a pressure vessel which allowed operation at pressures up to 4 bar. The test data were obtained using cosmic ray muons and a 1.5 GeV electron test beam.

3.1. First test module

In the first test module all wires were parallel. The 59 sense wires (gold-plated tungsten, 25 μm diameter) were arranged in 7 layers: 3 layers with field wires (Cu–Be, 75 μm diameter) between the sense wires and 4 layers without field wires. The cathode planes consisted of 75 μm diameter Cu–Be wires at a spacing of 1.4 mm. The cell size was 4.0×4.2 mm^2.

The main goal of these tests was the investigation of small drift cells in general, and the comparison of cells with and without field wires. Most tests were performed with a gas mixture of 80% CO_2 and 20% propane at pressures of 2, 3 and 4 bar.

Straight tracks in this test module are described by the two parameters d_0 (distance to the origin) and ϕ (azimuthal angle). For each event these are obtained by fitting calculated distances of closest approach to the measured drift distances. The drift distances are obtained from the measured TDC counts by means of the drift-time space relation (DTSR). The fit weights (for 10 ns intervals) are derived from the resolution function. The same DTSR and resolution function is used for all cells of the same type.

The DTSR and resolution function are determined in an iterative calibration procedure. Starting with reasonable approximations for both, a given data set is processed and distributions of residuals are accumulated. The residuals are defined as the difference between fitted and measured distances at the hit wires. They are biased towards smaller values because the measured distances serve as input to the track fit. In order to compensate for this, for a track with n hits all residuals are multiplied by a factor $k = \sqrt{n/(n-p)}$ (p = number of track parameters = 2). After the data are processed, the old value of the DTSR is corrected by the mean residual for a given drift time. The old value of the resolution function is replaced by the Gaussian standard deviation of the residual distribution in a given time interval. Then the data are processed again. This procedure is repeated until the DTSR and resolution function no longer change significantly. This calibration scheme converges quickly and has been successfully used for the ARGUS main and vertex drift chambers [2].

Far from the sense wire the isochrones deviate strongly from circles, especially in the drift cells without separating field wires (see fig. 3). Consequently, the drift distances depend on both the measured drift time and the track angle ϕ. Due to the limited statistics of the cosmic muon data sample collected with this test module it was not possible to fully map the two-dimensional DTSR. Instead, an empirical ϕ-correction (4th order polynomial) was iteratively determined and then applied to the drift distances calculated from the drift times alone.

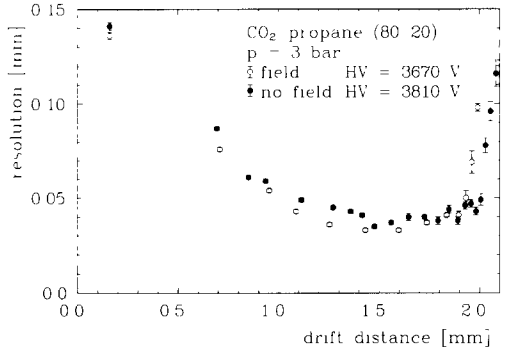

Fig. 5. Spatial resolution for cells with and without field wires in the first test module.

In fig. 5 the resolution functions are compared for drift cells with and without field wires, at an absolute pressure of 3 bar. There is no drastic difference in the performance of both cell types. The poor resolutions at large drift distances are due to the imperfect ϕ-correction. At a pressure of 4 bar the minimum resolution for cells without field wires is 25 μm.

Further improvement was achieved by performing an iterative least-squares fit of the wire positions, following the procedure outlined in ref. [7]. Within errors, the fitted wire positions were found to be independent of the analyzed data sample and of the operating conditions of the chamber. The resolution obtained with corrected wire positions at a pressure of 4 bar is shown in fig. 6. Combining this resolution function with the geometrical layer arrangement of the μVDC (see table 1), the mean impact parameter resolution at the beam line is 45 μm.

3.2. Second test module

The second test module incorporated some characteristic features of the μVDC design (see fig. 7). There are three pairs of layers with $\pm 45°$ stereo wires and

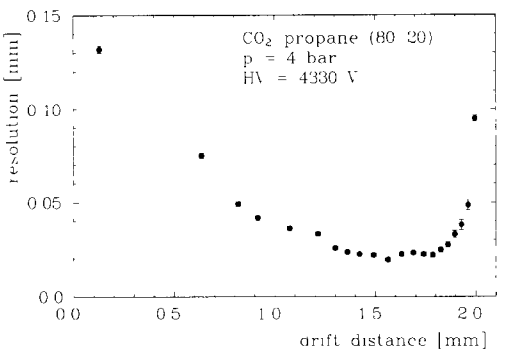

Fig. 6. Spatial resolution for cells without field wires with corrected wire positions in the first test module.

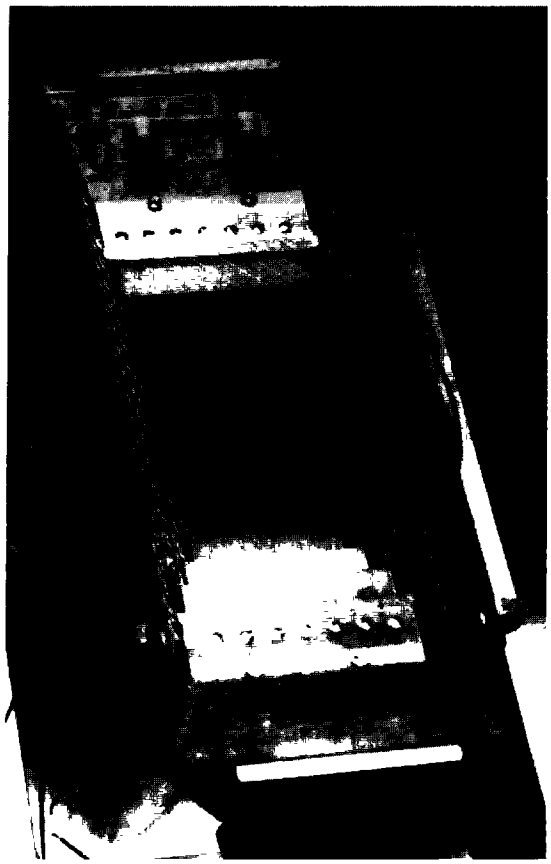

Fig. 7. The second μVDC test module Note the different orientations of sense wires in adjacent planes and the field shaping electrodes on the side walls

one layer of axial wires. The sense wires again are gold-plated tungsten wires with a diameter of 25 μm. There are no field wires separating the drift cells. The cells in this test module are slightly larger than in the first prototype, namely 5.0×5.1 mm^2. The cathode planes are made of axial Ni–Cr wires with 25 μm diameter at a spacing of 300 μm. The side walls of the test module, corresponding to the vanes in the μVDC, are covered with field shaping electrodes.

This test module is capable of a three-dimensional track measurement. A straight track in space is described by four parameters: d_0 and ϕ as described in the previous section, z_0 (z-coordinate of the point whose projection into the r–ϕ-plane has the distance d_0 from the origin), and θ (polar angle with respect to the z-axis). The data analysis followed the same general procedure as described in section 3.1.

However, it turned out that this test module was not suited for precise resolution studies because of the small number of layers for each stereo wire orientation. Therefore the main emphasis was put on the investigation of some other design features.

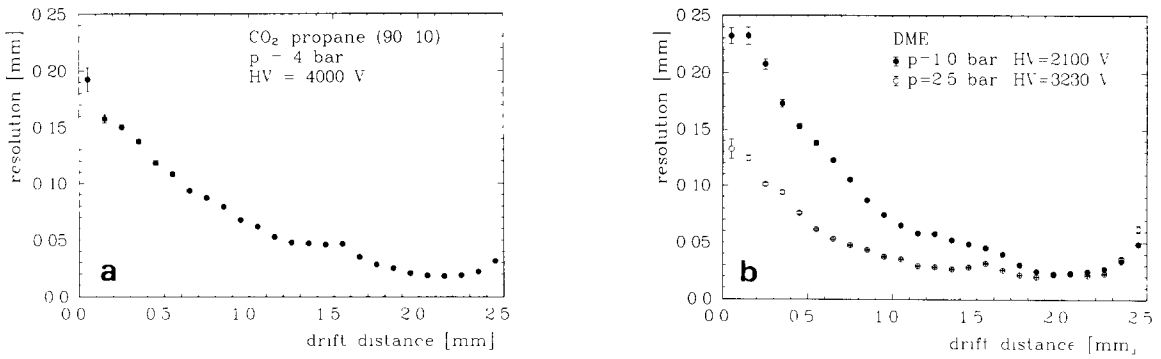

Fig. 8. Spatial resolution of the third test module at 30° deviation from perpendicular incidence on the sense wire planes. (a) CO_2/propane (90/10) at $p = 4$ bar; (b) pure DME at $p = 1$ and 2.5 bar.

Possible cross talk induced by the crossed anode and cathode wires was thoroughly investigated. Compared to the first test module, where all wires are parallel, no significantly different behaviour was observed.

The size of the inefficient regions close to the vanes was studied for various settings of the potentials on the field shaping electrodes. For the optimal choice of voltages the efficiency drops to 50% at about 0.5 mm from the vane.

In the electron test beam the ϕ-dependence of the drift–time space relation was mapped in 5° steps. In contrast with the analysis of the cosmic ray data, this allowed the investigation of the whole range of track angles with high statistics.

3.3. Third test module

A third test module [8] was designed to perform detailed resolution studies using different gas mixtures at various pressures. It consists of seven sense wire layers, each containing gold-plated tungsten wires of 20 μm diameter. There are no field wires between the sense wires. The sense wire layers are separated by cathode layers, consisting of nickel–chromium wires, 25 μm in diameter, with a spacing of 300 μm. The dimensions of the drift cells are 4.8×4.8 mm^2. All wires are parallel and 128 mm long. For these tests a prototype version of the new μVDC readout electronics described in section 2.6 was used.

The analysis of the test measurements followed the general scheme as described in section 3.1, except that, in order to avoid a bias, the layer used for calculating a residual was excluded from the track fit. In this case the error σ_{fit} of the distance of closest approach, obtained from the track fit, and the spatial resolution σ_r add quadratically to yield the width σ_{res} of the residual distribution. Therefore each residual is multiplied by a factor $1/\sqrt{1 + \sigma_{\text{fit}}^2/\sigma_r^2}$ with σ_r taken from the last iteration. When the iterative procedure has converged, the distribution of the corrected residuals yields the width σ_r. The resolution is determined for 100 μm intervals of the drift distance.

Measurements were performed with the angle of incidence of the electron beam varying in steps of 10°. Therefore it was possible to determine the drift–time space relation and the resolution function separately for each angle.

For straight tracks in the μVDC, the maximum possible angular deviation from perpendicular incidence on the sense wire planes is 36° (see fig. 1). The resolution obtained for a deviation of 30°, using a mixture of 90% CO_2 and 10% propane at a pressure of 4 bar, is shown in fig. 8a. Fig. 8b shows the results for pure dimethylether (DME) at 1 and 2.5 bar.

4. Conclusions

The main design features of the ARGUS μVDC are low multiple scattering, equal resolution in r–ϕ and r–z, and track coordinate measurements close to the beam line. This is realized by means of ±45° stereo wires, wound on a mechanical support structure, and by using a small diameter beryllium beam pipe. Several design details have been investigated using three different test modules. In particular it was shown that resolutions down to 20 μm can be obtained using pressurized cool gases, even for small drift cells without separating field wires. In order to operate the chamber under storage ring conditions, electronics with an efficient noise suppression scheme has been developed. First data from the μVDC in ARGUS are expected by the end of 1989.

Acknowledgements

For valuable contributions to the design and construction of the μVDC we thank Z. Arzoumanian, L.

Boissonneault, P. Charette, W. Cowan, P. Herman, A. Peter, A.A. Raffler and H. Rose from the Instrumentation Group and the Science Technology Center at Carleton University, Ottawa; C.E.K. Charlesworth and A. Kiang from the University of Toronto; N. Koch and P. Vaupel from the University of Dortmund; M. Hoffmann and M. Wagner from DESY. For the support during the test beam measurements we like to thank the staff at the Bonn University Synchrotron.

References

[1] H. Albrecht et al. (ARGUS Collaboration), DESY F15-86-01, August 1986.

[2] H. Albrecht et al. (ARGUS Collaboration), Nucl. Instr. and Meth. A275 (1989) 1.

[3] H. Albrecht et al. (ARGUS Collaboration), Phys. Lett. 185B (1987) 218.

[4] J. Huth and D. Nygren, Nucl. Instr. and Meth. A241 (1985) 375.

[5] E. Roderburg et al., Nucl. Instr. and Meth. A252 (1986) 285.

[6] V. Commichau et al., Nucl. Instr. and Meth. A239 (1985) 487.

[7] D.E. Amidei, Ph.D. Thesis, LBL-17795.

[8] T. Siegmund, Diploma thesis, University of Dortmund, January 1989.